Journal of Systems Engineering and Electronics
Vol. 31, No. 5, October 2020, pp.996 – 1008

Optimal observation configuration of UAVs based on angle and range measurements and cooperative target tracking in three-dimensional space

SHI Haoran, LU Faxing*, WANG Hangyu, and XU Junfei

College of Weaponry Engineering, Naval University of Engineering, Wuhan 430033, China

Abstract: This article investigates the optimal observation configuration of unmanned aerial vehicles (UAVs) based on angle and range measurements, and generalizes predecessors' researches in two dimensions into three dimensions. The relative geometry of the UAVs-target will significantly affect the state estimation performance of the target, the cost function based on the Fisher information matrix (FIM) is used to derive the FIM determinant of UAVs' observation in three-dimensional space, and the optimal observation geometric configuration that maximizes the determinant of the FIM is obtained. It is shown that the optimal observation configuration of the UAVs-target is usually not unique, and the optimal observation configuration is proved for two UAVs and three UAVs in three-dimension. The long-range over-the-horizon target tracking is simulated and analyzed based on the analysis of optimal observation configuration for two UAVs. The simulation results show that the theoretical analysis and control algorithm can effectively improve the positioning accuracy of the target. It can provide a helpful reference for the design of over-the-horizon target localization based on UAVs.

Keywords: target state estimation, optimal observation configuration, Fisher information matrix (FIM), Cramer-Rao lower bound (CRLB).

DOI: 10.23919/JSEE.2020.000074

1. Introduction

In recent years, unmanned aerial vehicles (UAVs) have been widely used in military and civilian applications due to their diverse sensors, concealed actions, controllable costs, and no need for personnel to come forward. In particular, they have the characteristics of aerial reconnaissance, so that UAVs have the potential to provide precise target position for long-range strike weapons [1,2].

Target localization and tracking have been studied extensively in numerous references. Xu and Shao et al. [3,4] studied the factors that affect the precise localization by UAVs, the main influencing factors include the position of the UAV, the navigation accuracy of the attitude angle and the relative position relationship between the UAV and the target. In the research of multi-UAV coordinated localization and tracking, in order to achieve the purpose of effectively using observation information [5], Campbell et al. [6] used unscented Kalman filtering combined with information filtering to fuse target state estimation, Wang et al. [7] used distributed unscented information filtering to achieve estimation of targets, and Yu et al. [8] used the two-level localization mode of coarse and fine to obtain the optimal solution of the target position.

However, the fusion filtering method is the only way to improve the target state estimation based on the observation data, the validity of the observation data varies according to the geometry of the UAV relative to the target. Subsequent research of relevance focuses mainly on developing methods for optimizing observation configuration to achieve the best target estimation performance. A common approach is to use objective functions derived from the determinant of the Fisher information matrix (FIM) [9 – 11]. FIM characterizes the amount of information about state parameters contained in a given observation sequence. The larger the value, the smaller covariance of the state estimation and the more accurate of the target state estimation. Tichavsky et al. [12] proposed a recursive FIM calculation method. Adrian et al. [13] studied the optimal sensor-target geometries for range-only, time-of-arrival-based and bearing-only localization. Sameera et al. [14] gave an FIM expression based on angle-measuring of UAVs system in three dimensions but did not simplify it. For a target-tracking application with range sensors, the determinant of the FIM is computed in the two-dimension (2-D) and three-dimension (3-D) cases by Sonia et al. [15].

Manuscript received January 02, 2020.
*Corresponding author.
This work was supported by the National Natural Science Foundation of China (61703419).

Eric et al. [16] researched the optimal observation configuration of double UAVs based on angle and range measurements in two-dimensional space. Wang [17] gave the determinant of FIM based on angle and range information in two dimensions and proposed the optimal observation configuration of UAVs. Zhong et al. [18] analyzed the optimal configuration of sensor-target geometries for bearing-only passive localization in three-dimensional space and theoretically derived it. Similar optimization functions are considered in some researches. Logothetis et al. [19] used mutual information as the objective function to model the optimal observational motion problem as a part of a considerable Markov process. Frew [20] explored the problem of trajectory planning for a 2-D ground robot equipped with vision sensors, using the determinant of the error covariance matrix as the objective function. The target tracking problem was solved by using the trace of the FIM as the objective function by Zhou et al. [21].

At present, most researches about the problem of coordinated localization and tracking of UAVs are based on short-range tracking, but there is little research on over-the-horizon target tracking by UAVs. Some researches with the optimal configuration of UAVs are in two-dimensional space, and some only consider the measurements of range-only or bearing-only in three-dimensional space, which is difficult to meet the requirements of accurate localization of the over-the-horizon target. For those reasons, this work builds upon previous literature by developing a cost function based on the determinant of FIM for designing UAVs observation configuration to localize a target using range and angle measurements in three-dimensional space. The purpose of this article is to focus on analyzing the optimal configuration of UAVs based on range and angle measurements, increasing the information provided by the measurements, reducing the uncertainty of target state estimation, and improving the accuracy in localization of the target. The optimal observation control algorithm of two UAVs is designed and simulated based on the analysis of optimal observation configuration for two UAVs. The simulation results verify the effectiveness of the theoretical analysis and control algorithm in this paper.

2. Determinant of FIM

2.1 Definition of FIM

Error covariance is a common performance function of state estimation, which represents the uncertainty of state estimation, so the error covariance should be as small as possible.

The Cramer-Rao lower bound (CRLB) provides a lower bound on the covariance of the estimation. Moreover, CRLB is related to the inherent properties of the system and has nothing to do with the specific estimation algorithm. The mathematical expression of CRLB is

$$\boldsymbol{CRLB} \triangleq \boldsymbol{F}_k^{-1} \leqslant$$

$$\boldsymbol{P}_{k|k} = \mathrm{E}\{[\widehat{\boldsymbol{X}}_{k|k} - \boldsymbol{X}_k][\widehat{\boldsymbol{X}}_{k|k} - \boldsymbol{X}_k]^{\mathrm{T}}\} \tag{1}$$

where $\boldsymbol{P}_{k|k}$ denotes the covariance matrix of the estimation error, $\boldsymbol{X}_k$ is the state to be estimated, and $\widehat{\boldsymbol{X}}_{k|k}$ is the estimated value of $\boldsymbol{X}_k$ under the given measurement data. $\boldsymbol{F}$ represents FIM, which is the inverse of CRLB, and it represents the amount of information about the state parameters contained in a given observation sequence.

The determinant of FIM $\det(F(T))$ is inversely proportional to the uncertainty area of T, therefore the optimality analysis of sensor-target geometry is equal to maximizing $\det(F(T))$.

2.2 Calculation for the determinant of FIM

In three-dimensional space, the target locates in $\boldsymbol{T}(x_t, y_t, z_t)$, UAV i locates in $\boldsymbol{U}_i(x_i, y_i, z_i)$, UAV j locates in $\boldsymbol{U}_j(x_j, y_j, z_j)$, the angle of sight between UAVs and the target is θ_{ij}, which is shown in Fig. 1.

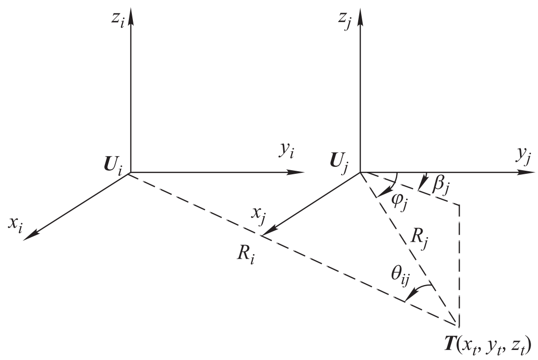

Fig. 1 Target localization by two UAVs

Fig. 1 shows the horizontal angle of the target observed by UAV j is β_j, and the pitch angle of the target observed by UAV j is φ_j. $\boldsymbol{X}_k = [x_t, y_t, z_t]_k^{\mathrm{T}}$ is the target state at time k, $\boldsymbol{U}_k = [x_u, y_u, z_u]_k^{\mathrm{T}}$ is the UAV state at time k, and the related vector between the UAV and the target is $\boldsymbol{r}_k = [r_x, r_y, r_z]_k^{\mathrm{T}}$, where $r_x = x_u - x_t$, $r_y = y_u - y_t$, $r_z = z_u - z_t$. We can obtain

$$\begin{cases} \sin\beta_j = \dfrac{r_x}{\sqrt{r_x^2 + r_y^2}} \\ \cos\beta_j = \dfrac{r_y}{\sqrt{r_x^2 + r_y^2}} \\ \sin\varphi_j = \dfrac{r_z}{\sqrt{r_x^2 + r_y^2 + r_z^2}} \\ \cos\varphi_j = \dfrac{\sqrt{r_x^2 + r_y^2}}{\sqrt{r_x^2 + r_y^2 + r_z^2}} \end{cases} . \tag{2}$$

The target information observed by the UAV is

$$\boldsymbol{h}(\boldsymbol{X}_k)=\begin{bmatrix} r & \beta & \varphi \end{bmatrix}^{\mathrm{T}}=\left[\begin{matrix}\sqrt{r_x^2+r_y^2+r_z^2} & \arctan\left(\dfrac{r_x}{r_y}\right) & \arctan\left(\dfrac{r_z}{\sqrt{r_x^2+r_y^2}}\right)\end{matrix}\right]^{\mathrm{T}}. \tag{3}$$

The Jacobian matrix of the observation function is expressed as

$$\boldsymbol{H}_k=\begin{bmatrix} \dfrac{r_x}{\sqrt{r_x^2+r_y^2+r_z^2}} & \dfrac{r_y}{\sqrt{r_x^2+r_y^2+r_z^2}} & \dfrac{r_z}{\sqrt{r_x^2+r_y^2+r_z^2}} \\ \dfrac{r_y}{r_x^2+r_y^2} & \dfrac{-r_x}{r_x^2+r_y^2} & 0 \\ \dfrac{-r_x r_z}{r_x^2+r_y^2+r_z^2\sqrt{r_x^2+r_y^2}} & \dfrac{-r_y r_z}{r_x^2+r_y^2+r_z^2\sqrt{r_x^2+r_y^2}} & \dfrac{\sqrt{r_x^2+r_y^2}}{r_x^2+r_y^2+r_z^2} \end{bmatrix}=[\boldsymbol{H}_r,\boldsymbol{H}_\beta,\boldsymbol{H}_\varphi]_k^{\mathrm{T}}. \tag{4}$$

e_{ri}, $e_{\beta i}$ and $e_{\varphi i}$ constitute the observation error matrix $\boldsymbol{R}_i$ of UAV i. $e_{ri}\sim N(0,\sigma_r^2)$, $e_{\beta i}\sim N(0,\sigma_\beta^2)$, $e_{\varphi i}\sim N(0,\sigma_\varphi^2)$. The observation error matrix of UAV i is

$$\boldsymbol{R}_i=\mathrm{diag}(\sigma_r^2,\sigma_\beta^2,\sigma_\varphi^2). \tag{5}$$

The FIM of this observation system [14] is

$$\boldsymbol{J}_k=[\boldsymbol{\Phi}_{k,k-1}^{\mathrm{T}}]^{-1}\boldsymbol{J}_{k-1}\boldsymbol{\Phi}_{k,k-1}^{-1}+\boldsymbol{H}_k^{\mathrm{T}}\boldsymbol{R}_k^{-1}\boldsymbol{H}_k. \tag{6}$$

In the optimal observation configuration, only the current position of the target is considered, and it is assumed that the current position of the target is fixed.

$$\boldsymbol{\Phi}_{k,k-1}=\begin{bmatrix}1&0&0\\0&1&0\\0&0&1\end{bmatrix} \tag{7}$$

Therefore, for the current UAV observation platforms, the total FIM of the system [17] can be expressed as

$$\boldsymbol{J}=\sum_{i=1}^{N}\boldsymbol{J}_i=\sum_{i=1}^{N}\boldsymbol{H}_i^{\mathrm{T}}\boldsymbol{R}_i\boldsymbol{H}_i=$$

$$\sum_{i=1}^{N}[\boldsymbol{H}_r,\boldsymbol{H}_\beta,\boldsymbol{H}_\varphi]_i\boldsymbol{R}_i\begin{bmatrix}\boldsymbol{H}_r\\\boldsymbol{H}_\beta\\\boldsymbol{H}_\varphi\end{bmatrix}_i^{\mathrm{T}}. \tag{8}$$

Assume that $\sigma^2=\sigma_\beta^2\cos^2\varphi=\sigma_\varphi^2$, and when UAVs observe a single target, the total FIM of the system is expressed as $\boldsymbol{J}=\boldsymbol{J}_N\boldsymbol{J}_N^{\mathrm{T}}$, where

$$\boldsymbol{J}_N=\left[\begin{matrix} \dfrac{\cos\varphi_1\sin\beta_1}{\sigma_r} & \dfrac{\cos\varphi_2\sin\beta_2}{\sigma_r} & \cdots & \dfrac{\cos\varphi_N\sin\beta_N}{\sigma_r} & \dfrac{\cos\beta_1}{\sigma R_1} & \dfrac{\cos\beta_2}{\sigma R_2} & \cdots & \dfrac{\cos\beta_N}{\sigma R_N} \\ \dfrac{\cos\varphi_1\cos\beta_1}{\sigma_r} & \dfrac{\cos\varphi_2\cos\beta_2}{\sigma_r} & \cdots & \dfrac{\cos\varphi_N\cos\beta_N}{\sigma_r} & -\dfrac{\sin\beta_1}{\sigma R_1} & -\dfrac{\sin\beta_2}{\sigma R_2} & \cdots & -\dfrac{\sin\beta_N}{\sigma R_N} \\ \dfrac{\sin\varphi_1}{\sigma_r} & \dfrac{\sin\varphi_2}{\sigma_r} & \cdots & \dfrac{\sin\varphi_N}{\sigma_r} & 0 & 0 & \cdots & 0 \end{matrix}\right.$$

$$\left.\begin{matrix} -\dfrac{\sin\beta_1\sin\varphi_1}{\sigma R_1} & -\dfrac{\sin\beta_2\sin\varphi_2}{\sigma R_2} & \cdots & -\dfrac{\sin\beta_N\sin\varphi_N}{\sigma R_N} \\ -\dfrac{\cos\beta_1\sin\varphi_1}{\sigma R_1} & -\dfrac{\cos\beta_2\sin\varphi_2}{\sigma R_2} & \cdots & -\dfrac{\cos\beta_N\sin\varphi_N}{\sigma R_N} \\ \dfrac{\cos\varphi_1}{\sigma R_1} & \dfrac{\cos\varphi_2}{\sigma R_2} & \cdots & \dfrac{\cos\varphi_N}{\sigma R_N} \end{matrix}\right]. \tag{9}$$

Using the Cauchy-Binet [22] formula, $\det(\boldsymbol{J})$ is composed of the following ten parts, and the case of $N=2$ is explained at the same time.

(i) $\sum\limits_{S_1}\det(\boldsymbol{D}_1)\cdot\det(\boldsymbol{D}_1^{\mathrm{T}})$, $N(S_1)=\mathrm{C}_N^1\mathrm{C}_N^1\mathrm{C}_N^1$, S_1 represents a subset, $\boldsymbol{D}_1$ is a block matrix of 3 times 3, $N(S_1)$ represents the number of elements contained in S_1, with the same meaning later.

$$\boldsymbol{D}_1=\begin{bmatrix} \dfrac{\cos\varphi_i\sin\beta_i}{\sigma_r} & \dfrac{\cos\beta_j}{\sigma R_j} & -\dfrac{\sin\beta_k\sin\varphi_k}{\sigma R_k} \\ \dfrac{\cos\varphi_i\cos\beta_i}{\sigma_r} & -\dfrac{\sin\beta_j}{\sigma R_j} & -\dfrac{\cos\beta_k\sin\varphi_k}{\sigma R_k} \\ \dfrac{\sin\varphi_i}{\sigma_r} & 0 & \dfrac{\cos\varphi_k}{\sigma R_k} \end{bmatrix} \tag{10}$$

i) As $i=j=k$, that is i, j, k columns of observation come from the same UAV, this sub-part is equal to

$$\sum_{S_{11}} \det(\boldsymbol{D}_1)\cdot\det(\boldsymbol{D}_1^{\mathrm{T}}) = \sum_{S_{11}} \frac{1}{\sigma_r^2\sigma^4 R_j^4} \tag{11}$$

where $S_{11}=\{(i,j,k)|1\leqslant i=j=k\leqslant N\}$, $N(S_{11})=\mathrm{C}_N^1$.

ii) As $i=j\neq k$, both columns i and j come from the same UAV, column k comes from another UAV, this sub-part is equal to

$$\sum_{S_{12}} \det(\boldsymbol{D}_1)\cdot\det(\boldsymbol{D}_1^{\mathrm{T}}) =$$

$$\sum_{S_{12}} \frac{[\sin\varphi_i\sin\varphi_k\cos(\beta_i-\beta_k)+\cos\varphi_i\cos\varphi_k]^2}{\sigma_r^2\sigma^4 R_i^2 R_k^2} \tag{12}$$

where $S_{12}=\{(i,j,k)|1\leqslant i=j\neq k\leqslant N\}$, $N(S_{12})=\mathrm{C}_N^1\mathrm{C}_{N-1}^1$.

iii) As $i=k\neq j$, both columns i and k come from the same UAV, column j comes from another UAV, this sub-part is equal to

$$\sum_{S_{13}} \det(\boldsymbol{D}_1)\cdot\det(\boldsymbol{D}_1^{\mathrm{T}}) = \sum_{S_{13}} \frac{\cos^2(\beta_i-\beta_j)}{\sigma_r^2\sigma^4 R_i^2 R_j^2} \tag{13}$$

where $S_{13}=\{(i,j,k)|1\leqslant i=k\neq j\leqslant N\}$, $N(S_{13})=\mathrm{C}_N^1\mathrm{C}_{N-1}^1$.

iv) As $i\neq j=k$, both columns j and k come from the same UAV, column i comes from another UAV, this sub-part is equal to

$$\sum_{S_{14}} \det(\boldsymbol{D}_1)\cdot\det(\boldsymbol{D}_1^{\mathrm{T}}) =$$

$$\sum_{S_{14}} \frac{[\cos\varphi_i\cos\varphi_k\cos(\beta_i-\beta_k)+\sin\varphi_i\sin\varphi_k]^2}{\sigma_r^2\sigma^4 R_i^2} \tag{14}$$

where $S_{14}=\{(i,j,k)|1\leqslant i\neq j=k\leqslant N\}$, $N(S_{14})=\mathrm{C}_N^1\mathrm{C}_{N-1}^1$.

v) As $i\neq j\neq k$, columns i, j and k come from different UAVs, this sub-part is equal to

$$\sum_{S_{15}} \det(\boldsymbol{D}_1)\cdot\det(\boldsymbol{D}_1^{\mathrm{T}}) = \sum_{S_{15}} \frac{[\cos\varphi_i\cos\varphi_k\cos(\beta_i-\beta_j)+\sin\varphi_i\sin\varphi_k\cos(\beta_j-\beta_k)]^2}{\sigma_r^2\sigma^4 R_j^2 R_k^2} \tag{15}$$

where $S_{15}=\{(i,j,k)|1\leqslant i\neq j\neq k\leqslant N\}$, $N(S_{15})=\mathrm{C}_N^1\mathrm{C}_{N-1}^1\mathrm{C}_{N-2}^1$. In the case of $N=2$, this part does not exist. $S_1=S_{11}\cup S_{12}\cup S_{13}\cup S_{14}\cup S_{15}$, the first part is equal to the sum of (11)–(15).

(ii) $\sum\limits_{S_2}\det(\boldsymbol{D}_2)\cdot\det(\boldsymbol{D}_2^{\mathrm{T}})$, $N(S_2)=\mathrm{C}_N^1\mathrm{C}_N^2$.

$$\boldsymbol{D}_2=\begin{bmatrix} \dfrac{\cos\varphi_i\sin\beta_i}{\sigma_r} & \dfrac{\cos\beta_j}{\sigma R_j} & \dfrac{\cos\varphi_k\sin\beta_k}{\sigma_r} \\ \dfrac{\cos\varphi_i\cos\beta_i}{\sigma_r} & -\dfrac{\sin\beta_j}{\sigma R_j} & \dfrac{\cos\varphi_k\cos\beta_k}{\sigma_r} \\ \dfrac{\sin\varphi_i}{\sigma_r} & 0 & \dfrac{\sin\varphi_k}{\sigma_r} \end{bmatrix} \tag{16}$$

i) As $i=j$, both columns i and j come from the same UAV, this sub-part is equal to

$$\sum_{S_{21}} \det(\boldsymbol{D}_2)\cdot\det(\boldsymbol{D}_2^{\mathrm{T}}) =$$

$$\sum_{S_{21}} \frac{[\sin\varphi_j\cos\varphi_k\cos(\beta_j-\beta_k)-\cos\varphi_j\sin\varphi_k]^2}{\sigma_r^4\sigma^2 R_j^2} \tag{17}$$

where $S_{21}=\{(j,k)|1\leqslant j<k\leqslant N\}$, $N(S_{21})=\mathrm{C}_N^2$.

ii) As $j=k$, both columns j and k come from the same UAV, this sub-part is equal to

$$\sum_{S_{22}} \det(\boldsymbol{D}_2)\cdot\det(\boldsymbol{D}_2^{\mathrm{T}}) =$$

$$\sum_{S_{22}} \frac{[\sin\varphi_j\cos\varphi_i\cos(\beta_i-\beta_j)-\cos\varphi_j\sin\varphi_i]^2}{\sigma_r^4\sigma^2 R_j^2} \tag{18}$$

where $S_{22}=\{(i,j)|1\leqslant i<j\leqslant N\}$, $N(S_{22})=\mathrm{C}_N^2$.

iii) As $i\neq j\neq k$, columns i, j and k come from different UAVs, this sub-part is equal to

$$\sum_{S_{23}} \det(\boldsymbol{D}_2)\cdot\det(\boldsymbol{D}_2^{\mathrm{T}}) = \sum_{S_{23}} \frac{[\sin\varphi_i\cos\varphi_k\cos(\beta_j-\beta_k)-\cos\varphi_i\sin\varphi_k\cos(\beta_i-\beta_j)]^2}{\sigma_r^4\sigma^2 R_j^2} \tag{19}$$

where $S_{23}=\{(i,j,k)|1\leqslant i<k\leqslant N, 1\leqslant j\leqslant N, j\neq i, j\neq k\}$, $N(S_{23})=\mathrm{C}_N^2\mathrm{C}_{N-2}^1$, in the case of $N=2$, this part does not exist.

(iii) $\sum\limits_{S_3}\det(\boldsymbol{D}_3)\cdot\det(\boldsymbol{D}_3^{\mathrm{T}})$, $N(S_3)=\mathrm{C}_N^1\mathrm{C}_N^2$.

$$\boldsymbol{D}_3=\begin{bmatrix}\dfrac{\cos\varphi_i\sin\beta_i}{\sigma_r} & \dfrac{\cos\beta_j}{\sigma R_j} & \dfrac{\cos\beta_k}{\sigma R_k}\\ \dfrac{\cos\varphi_i\cos\beta_i}{\sigma_r} & -\dfrac{\sin\beta_j}{\sigma R_j} & -\dfrac{\sin\beta_k}{\sigma R_k}\\ \dfrac{\sin\varphi_i}{\sigma_r} & 0 & 0\end{bmatrix} \tag{20}$$

Similar to the analysis of the second part, the third part is also divided into three situations. The third part is as follows:

$$\sum_{S_3}\det(\boldsymbol{D}_3)\cdot\det(\boldsymbol{D}_3^{\mathrm{T}})=\sum_{S_{31}}\frac{\sin^2\varphi_j\sin^2(\beta_j-\beta_k)}{\sigma_r^2\sigma^4R_j^2R_k^2}+\sum_{S_{32}}\frac{\sin^2\varphi_k\sin^2(\beta_j-\beta_k)}{\sigma_r^2\sigma^4R_j^2R_k^2}+\sum_{S_{33}}\frac{\sin^2\varphi_i\sin^2(\beta_k-\beta_j)}{\sigma_r^2\sigma^4R_j^2R_k^2} \tag{21}$$

where $S_{31}=\{(j,k)|1\leqslant j<k\leqslant N\}$, $N(S_{31})=\mathrm{C}_N^2$, $S_{32}\triangleq S_{31}$, $S_{33}=\{(i,j,k)|1\leqslant j<k\leqslant 2,1\leqslant i\leqslant 2,i\neq j,i\neq k\}$, $N(S_{33})=\mathrm{C}_N^2\mathrm{C}_{N-2}^1$. In the case of $N=2$, the last sub-part does not exist.

(iv) $\sum_{S_4}\det(\boldsymbol{D}_4)\cdot\det(\boldsymbol{D}_4^{\mathrm{T}})$, $N(S_4)=\mathrm{C}_N^1\mathrm{C}_N^2$.

$$\boldsymbol{D}_4=\begin{bmatrix}\dfrac{\cos\varphi_i\sin\beta_i}{\sigma_r} & -\dfrac{\sin\beta_j\sin\varphi_j}{\sigma R_j} & \dfrac{\cos\varphi_k\sin\beta_k}{\sigma_r}\\ \dfrac{\cos\varphi_i\cos\beta_i}{\sigma_r} & -\dfrac{\cos\beta_j\sin\varphi_j}{\sigma R_j} & \dfrac{\cos\varphi_k\cos\beta_k}{\sigma_r}\\ \dfrac{\sin\varphi_i}{\sigma_r} & \dfrac{\cos\varphi_j}{\sigma R_j} & \dfrac{\sin\varphi_k}{\sigma_r}\end{bmatrix} \tag{22}$$

Similar to the analysis of the second part, the fourth part is also divided into three situations. The fourth part is as follows:

$$\sum_{S_4}\det(\boldsymbol{D}_4)\cdot\det(\boldsymbol{D}_4^{\mathrm{T}})=\sum_{S_{41}}\frac{\cos^2\varphi_k\sin^2(\beta_j-\beta_k)}{\sigma_r^4\sigma^2R_j^2}+\sum_{S_{42}}\frac{\cos^2\varphi_i\sin^2(\beta_i-\beta_j)}{\sigma_r^4\sigma^2R_j^2}+\sum_{S_{43}}\frac{[\sin\varphi_i\sin\varphi_j\cos\varphi_k\sin(\beta_j-\beta_k)+\cos\varphi_i\cos\varphi_j\cos\varphi_k\sin(\beta_i-\beta_k)+\cos\varphi_i\sin\varphi_j\sin\varphi_k\sin(\beta_i-\beta_j)]^2}{\sigma_r^4\sigma^2R_j^2} \tag{23}$$

where

$$S_{41}=\{(j,k)|1\leqslant j<k\leqslant N\},N(S_{41})=\mathrm{C}_N^2,$$

$$S_{42}=\{(i,j)|1\leqslant i<j\leqslant N\},N(S_{42})=\mathrm{C}_N^2,$$

$S_{43}=\{(i,j,k)|1\leqslant i<k\leqslant N,1\leqslant j\leqslant N,i\neq j,j\neq k\}$, $N(S_{43})=\mathrm{C}_N^2\mathrm{C}_{N-2}^1$. In the case of $N=2$, the last sub-part does not exist.

(v) $\sum_{S_5}\det(\boldsymbol{D}_5)\cdot\det(\boldsymbol{D}_5^{\mathrm{T}})$, $N(S_5)=\mathrm{C}_N^1\mathrm{C}_N^2$.

$$\boldsymbol{D}_5=\begin{bmatrix}\dfrac{\cos\varphi_i\sin\beta_i}{\sigma_r} & -\dfrac{\sin\beta_j\sin\varphi_j}{\sigma R_j} & -\dfrac{\sin\beta_k\sin\varphi_k}{\sigma R_k}\\ \dfrac{\cos\varphi_i\cos\beta_i}{\sigma_r} & -\dfrac{\cos\beta_j\sin\varphi_j}{\sigma R_j} & -\dfrac{\cos\beta_k\sin\varphi_k}{\sigma R_k}\\ \dfrac{\sin\varphi_i}{\sigma_r} & \dfrac{\cos\varphi_j}{\sigma R_j} & \dfrac{\cos\varphi_k}{\sigma R_k}\end{bmatrix} \tag{24}$$

Similar to the analysis of the second part, the fifth part is also divided into three situations. The fifth part is as follows:

$$\sum_{S_5}\det(\boldsymbol{D}_5)\cdot\det(\boldsymbol{D}_5^{\mathrm{T}})=\sum_{S_{51}}\frac{\cos^2\varphi_k\sin^2(\beta_j-\beta_k)}{\sigma_r^2\sigma^4R_j^2R_k^2}+\sum_{S_{52}}\frac{\cos^2\varphi_j\sin^2(\beta_k-\beta_j)}{\sigma_r^2\sigma^4R_j^2R_k^2}+\sum_{S_{53}}\frac{[\sin\varphi_i\sin\varphi_j\sin\varphi_k\sin(\beta_j-\beta_k)+\cos\varphi_i\cos\varphi_j\sin\varphi_k\sin(\beta_i-\beta_k)+\cos\varphi_i\sin\varphi_j\cos\varphi_k\sin(\beta_j-\beta_i)]^2}{\sigma_r^2\sigma^4R_j^2R_k^2} \tag{25}$$

where

$$S_{51}=\{(j,k)|1\leqslant j<k\leqslant N\},$$

$$N(S_{52})=\mathrm{C}_N^2,S_{52}\triangleq S_{51},$$

$S_{53}=\{(i,j,k)|1\leqslant j<k\leqslant N,1\leqslant i\leqslant N,i\neq j,i\neq k\}$, $N(S_{53})=\mathrm{C}_N^2\mathrm{C}_{N-2}^1$. In the case of $N=2$, the last sub-part does not exist.

(vi) $\sum_{S_6}\det(\boldsymbol{D}_6)\cdot\det(\boldsymbol{D}_6^{\mathrm{T}})$, $N(S_6)=\mathrm{C}_N^1\mathrm{C}_N^2$.

$$\boldsymbol{D}_6=\begin{bmatrix}\dfrac{\cos\beta_i}{\sigma R_i} & \dfrac{\cos\beta_j}{\sigma R_j} & -\dfrac{\sin\beta_k\sin\varphi_k}{\sigma R_k}\\ -\dfrac{\sin\beta_i}{\sigma R_i} & -\dfrac{\sin\beta_j}{\sigma R_j} & -\dfrac{\cos\beta_k\sin\varphi_k}{\sigma R_k}\\ 0 & 0 & \dfrac{\cos\varphi_k}{\sigma R_k}\end{bmatrix} \tag{26}$$

Similar to the analysis of the second part, the sixth part is also divided into three situations. The sixth part is as follows:

$$\sum_{S_6}\det(\boldsymbol{D}_6)\cdot\det(\boldsymbol{D}_6^{\mathrm{T}})=\sum_{S_{61}}\frac{\cos^2\varphi_i\sin^2(\beta_i-\beta_j)}{\sigma^6R_i^4R_j^2}+\sum_{S_{62}}\frac{\cos^2\varphi_j\sin^2(\beta_i-\beta_j)}{\sigma^6R_i^2R_j^4}+\sum_{S_{63}}\frac{\cos^2\varphi_k\sin^2(\beta_i-\beta_j)}{\sigma^6R_i^2R_j^2R_k^2} \tag{27}$$

where $S_{61}=\{(i,j)|1\leqslant i<j\leqslant N\}$, $N(S_{61})=\mathrm{C}_N^2$, $S_{62}\triangleq S_{61}$, $S_{63}=\{(i,j,k)|1\leqslant i<j\leqslant N, 1\leqslant k\leqslant N, i\neq k, j\neq k\}$, $N(S_{63})=\mathrm{C}_N^2\mathrm{C}_{N-2}^1$. In the case of $N=2$, the last sub-part does not exist.

(vii) $\sum\limits_{S_7}\det(\boldsymbol{D}_7)\cdot\det(\boldsymbol{D}_7^{\mathrm{T}})$, $N(S_7)=\mathrm{C}_N^1\mathrm{C}_N^2$.

$$\boldsymbol{D}_7=\begin{bmatrix}\dfrac{\cos\beta_i}{\sigma R_i} & -\dfrac{\sin\beta_j\sin\varphi_j}{\sigma R_j} & -\dfrac{\sin\beta_k\sin\varphi_k}{\sigma R_k}\\ -\dfrac{\sin\beta_i}{\sigma R_i} & -\dfrac{\cos\beta_j\sin\varphi_j}{\sigma R_j} & -\dfrac{\cos\beta_k\sin\varphi_k}{\sigma R_k}\\ 0 & \dfrac{\cos\varphi_j}{\sigma R_j} & \dfrac{\cos\varphi_k}{\sigma R_k}\end{bmatrix} \tag{28}$$

Similar to the analysis of the second part, the seventh part is also divided into three situations. The seventh part is as follows:

$$\sum_{S_7}\det(\boldsymbol{D}_7)\cdot\det(\boldsymbol{D}_7^{\mathrm{T}})=\sum_{S_{71}}\frac{[\cos\varphi_j\sin\varphi_k\cos(\beta_j-\beta_k)-\sin\varphi_j\cos\varphi_k]^2}{\sigma^6R_j^4R_k^2}+\sum_{S_{72}}\frac{[\sin\varphi_j\cos\varphi_k\cos(\beta_j-\beta_k)-\cos\varphi_j\sin\varphi_k]^2}{\sigma^6R_j^2R_k^4}+\sum_{S_{73}}\frac{[\cos\varphi_j\sin\varphi_k\cos(\beta_i-\beta_k)-\sin\varphi_j\cos\varphi_k\cos(\beta_i-\beta_j)]^2}{\sigma^6R_i^2R_j^2R_k^2} \tag{29}$$

where $S_{71}=\{(j,k)|1\leqslant j<k\leqslant N\}$, $N(S_{71})=\mathrm{C}_N^2$, $S_{72}\triangleq S_{71}$, $S_{73}=\{(i,j,k)|1\leqslant j<k\leqslant N, 1\leqslant i\leqslant N, i\neq j, i\neq k\}$, $N(S_{73})=\mathrm{C}_N^2\mathrm{C}_{N-2}^1$. In the case of $N=2$, the last sub-part does not exist.

(viii) $\sum\limits_{S_8}\det(\boldsymbol{D}_8)\cdot\det(\boldsymbol{D}_8^{\mathrm{T}})$, $N(S_8)=\mathrm{C}_N^3$.

$$\boldsymbol{D}_8=\begin{bmatrix}\dfrac{\cos\beta_i}{\sigma R_i} & \dfrac{\cos\beta_j}{\sigma R_j} & \dfrac{\cos\beta_k}{\sigma R_k}\\ -\dfrac{\sin\beta_i}{\sigma R_i} & -\dfrac{\sin\beta_j}{\sigma R_j} & -\dfrac{\sin\beta_k}{\sigma R_k}\\ 0 & 0 & 0\end{bmatrix} \tag{30}$$

This part is equal to zero.

(ix) $\sum\limits_{S_9}\det(\boldsymbol{D}_9)\cdot\det(\boldsymbol{D}_9^{\mathrm{T}})$, $N(S_9)=\mathrm{C}_N^3$.

$$\boldsymbol{D}_9=\begin{bmatrix}\dfrac{\cos\varphi_i\sin\beta_i}{\sigma_r} & \dfrac{\cos\varphi_j\sin\beta_j}{\sigma_r} & \dfrac{\cos\varphi_k\sin\beta_k}{\sigma_r}\\ \dfrac{\cos\varphi_i\cos\beta_i}{\sigma_r} & \dfrac{\cos\varphi_j\cos\beta_j}{\sigma_r} & \dfrac{\cos\varphi_k\cos\beta_k}{\sigma_r}\\ \dfrac{\sin\varphi_i}{\sigma_r} & \dfrac{\sin\varphi_j}{\sigma_r} & \dfrac{\sin\varphi_k}{\sigma_r}\end{bmatrix} \tag{31}$$

As $i\neq j\neq k$, columns i, j and k come from different UAVs, this part is equal to

$$\sum_{S_9}\det(\boldsymbol{D}_9)\cdot\det(\boldsymbol{D}_9^{\mathrm{T}})=\sum_{S_9}\frac{[\sin\varphi_i\cos\varphi_j\cos\varphi_k\sin(\beta_j-\beta_k)+\cos\varphi_i\sin\varphi_j\cos\varphi_k\sin(\beta_k-\beta_i)+\cos\varphi_i\cos\varphi_j\sin\varphi_k\sin(\beta_i-\beta_j)]^2}{\sigma_r^6} \tag{32}$$

where $S_9=\{(i,j,k)|1\leqslant i<j<k\leqslant N\}$. In the case of $N=2$, this part does not exist.

(x) $\sum\limits_{S_{10}}\det(\boldsymbol{D}_{10})\cdot\det(\boldsymbol{D}_{10}^{\mathrm{T}})$, $N(S_{10})=\mathrm{C}_N^3$.

$$\boldsymbol{D}_{10}=\begin{bmatrix}-\dfrac{\sin\beta_i\sin\varphi_i}{\sigma R_i} & -\dfrac{\sin\beta_j\sin\varphi_j}{\sigma R_j} & -\dfrac{\sin\beta_k\sin\varphi_k}{\sigma R_k}\\ -\dfrac{\cos\beta_i\sin\varphi_i}{\sigma R_i} & -\dfrac{\cos\beta_j\sin\varphi_j}{\sigma R_j} & -\dfrac{\cos\beta_k\sin\varphi_k}{\sigma R_k}\\ \dfrac{\cos\varphi_i}{\sigma R_i} & \dfrac{\cos\varphi_j}{\sigma R_j} & \dfrac{\cos\varphi_k}{\sigma R_k}\end{bmatrix} \tag{33}$$

As $i \neq j \neq k$, columns i, j and k come from different UAVs, this part is equal to

$$\sum_{S_{10}} \det(\boldsymbol{D}_{10}) \cdot \det(\boldsymbol{D}_{10}^{\mathrm{T}}) =$$

$$\sum_{S_{10}} \frac{[\cos\varphi_i \sin\varphi_j \sin\varphi_k \sin(\beta_k-\beta_j) + \sin\varphi_i \cos\varphi_j \sin\varphi_k \sin(\beta_i-\beta_k) + \sin\varphi_i \sin\varphi_j \cos\varphi_k \sin(\beta_j-\beta_i)]^2}{\sigma^6 R_i^2 R_j^2 R_k^2} \quad (34)$$

where $S_{10} = \{(i,j,k) | 1 \leqslant i < j < k \leqslant N\}$. In the case of $N = 2$, this part does not exist.

2.3 Four equations used to compute the determinant of FIM

The following four equations are needed to calculate the FIM determinant of a system.

Given $\boldsymbol{r}(\varphi_i,\beta_i) = (\cos\varphi_i \sin\beta_i, \cos\varphi_i \cos\beta_i, \sin\varphi_i)$, we can get the followings:

(i) According to the definition of $\cos\theta_{ij}$ in Fig. 1,

$$\cos\theta_{ij} = \boldsymbol{r}(\varphi_i,\beta_i) \cdot \boldsymbol{r}(\varphi_j,\beta_j) =$$
$$\cos\varphi_i \cos\varphi_j \cos(\beta_j-\beta_i) + \sin\varphi_i \sin\varphi_j \quad (35)$$

where $1 \leqslant i < j \leqslant N$.

(ii) From (35), we can get

$$[\cos\varphi_j \sin\varphi_i - \sin\varphi_j \cos\varphi_i \cos(\beta_j-\beta_i)]^2 +$$
$$\cos^2\varphi_i \sin^2(\beta_j-\beta_i) = 1 - [r(\varphi_i,\beta_i) \cdot r(\varphi_j,\beta_j)]^2 =$$
$$1 - \cos^2\theta_{ij} \quad (36)$$

where $1 \leqslant i < j \leqslant N$.

(iii) Calculate the mixed product of $\boldsymbol{r}(\varphi_1,\beta_1)$, $\boldsymbol{r}(\varphi_2,\beta_2)$ and $\boldsymbol{r}(\varphi_3,\beta_3)$:

$$[\boldsymbol{r}(\varphi_1,\beta_1)\boldsymbol{r}(\varphi_2,\beta_2)\boldsymbol{r}(\varphi_3,\beta_3)]^2 =$$
$$[\sin\varphi_1 \cos\varphi_2 \cos\varphi_3 \sin(\beta_2-\beta_3) +$$
$$\cos\varphi_1 \sin\varphi_2 \cos\varphi_3 \sin(\beta_3-\beta_1) +$$
$$\cos\varphi_1 \cos\varphi_2 \sin\varphi_3 \sin(\beta_1-\beta_2)]^2. \quad (37)$$

(iv) There are the following relationships:

$$[\boldsymbol{r}(\varphi_1,\beta_1)\boldsymbol{r}(\varphi_2,\beta_2)\boldsymbol{r}(\varphi_3,\beta_3)]^2 =$$
$$1 - [\boldsymbol{r}(\varphi_1,\beta_1)\boldsymbol{r}(\varphi_2,\beta_2)]^2 - [\boldsymbol{r}(\varphi_1,\beta_1)\boldsymbol{r}(\varphi_3,\beta_3)]^2 -$$
$$[\boldsymbol{r}(\varphi_2,\beta_2)\boldsymbol{r}(\varphi_3,\beta_3)]^2 + 2[\boldsymbol{r}(\varphi_1,\beta_1)\boldsymbol{r}(\varphi_2,\beta_2)] \cdot$$
$$[\boldsymbol{r}(\varphi_1,\beta_1)\boldsymbol{r}(\varphi_3,\beta_3)][\boldsymbol{r}(\varphi_2,\beta_2)\boldsymbol{r}(\varphi_3,\beta_3)]. \quad (38)$$

3. Analysis of optimal observation configuration

The optimal observation configuration refers to UAVs observation configuration which minimizes the error of target state estimation. The quality of the measurement data is closely related to the observation position of the UAV relative to the target. The target information provided by the measurement data obtained from different observation positions is different. The “good” or “bad” of the measured data directly affects the target state estimation. This part mainly analyzes the observation configuration of the UAV, so that the UAV is in a better observation position and get a better target state estimation.

From the derivation process of FIM determinant, it can be seen that when moving UAV i from $\boldsymbol{U}_i = (x_{ui}, y_{ui}, z_{ui})$ to $\boldsymbol{U}_i' = (2x_t - x_{ui}, 2y_t - y_{ui}, z_{ui})$, the total determinant value of FIM does not change, so the optimal observation configuration of the UAVs is not unique.

3.1 Analysis of optimal observation configuration for $N = 1$

When $N = 1$, that is, a single UAV observes the target.

$$\boldsymbol{J}_1 = \begin{bmatrix} \dfrac{\cos\varphi_1 \sin\beta_1}{\sigma_r} & \dfrac{\cos\beta_1}{\sigma R_1} & -\dfrac{\sin\beta_1 \sin\varphi_1}{\sigma R_1} \\ \dfrac{\cos\varphi_1 \cos\beta_1}{\sigma_r} & -\dfrac{\sin\beta_1}{\sigma R_1} & -\dfrac{\cos\beta_1 \sin\varphi_1}{\sigma R_1} \\ \dfrac{\sin\varphi_1}{\sigma_r} & 0 & \dfrac{\cos\varphi_1}{\sigma R_1} \end{bmatrix} \quad (39)$$

The total determinant of FIM is

$$\det(\boldsymbol{J}) = \det(\boldsymbol{J}_1)\det(\boldsymbol{J}_1^{\mathrm{T}}) = \frac{1}{\sigma_r^2 \sigma^4 R_1^2}. \quad (40)$$

This shows that the smaller distance between the UAV and the target is, the larger determinant of the FIM is, and the more information UAV observes on the target, especially $R_1^2 \to 0$, $\det(\boldsymbol{J}) \to \infty$. Therefore, when a single UAV observes, it will shorten the distance between the UAV and the target as soon as possible. There is a minimum observation distance $r_{\min}$ in practical application, the maximum determinant value of the system FIM is $\det(\boldsymbol{J}) = 1/(\sigma_r^2 \sigma^4 r_{\min}^2)$. Especially $R_1^2 \to \infty$, $\det(\boldsymbol{J}) \to 0$, there is no unbiased estimator.

3.2 Analysis of optimal observation configuration for $N = 2$

When $N = 2$, that is, two UAVs observe a single target, the total determinant of FIM is

$$\det(\boldsymbol{J}_2) = \det(\boldsymbol{F}_2)\det(\boldsymbol{F}_2^{\mathrm{T}}) =$$
$$\frac{(1+\cos^2\theta_{12})}{\sigma_r^2\sigma^4}\left(\frac{1}{R_1^4}+\frac{1}{R_2^4}\right)+$$
$$\frac{(1-\cos^2\theta_{12})}{\sigma_r^4\sigma^2}\left(\frac{1}{R_1^2}+\frac{1}{R_2^2}\right)+$$
$$\frac{(1-\cos^2\theta_{12})}{\sigma^6}\left(\frac{1}{R_1^2R_2^4}+\frac{1}{R_1^4R_2^2}\right)+$$
$$\frac{2(1+\cos^2\theta_{12})}{\sigma_r^2\sigma^4R_1^2R_2^2}. \tag{41}$$

From (41), we can get when two UAVs observe, $R_i = r_{\min}$ $(i \in \{1,2\})$ is a necessary condition for the maximum determinant of FIM. When $R_1 = R_2 = r_{\min}$, then,

$$\det(\boldsymbol{J}_2) = \frac{2}{r_{\min}^6\sigma_r^4\sigma^6}[(r_{\min}^2\sigma^2+\sigma_r^2)^2-$$
$$(r_{\min}^2\sigma^2-\sigma_r^2)^2\cos^2\theta_{12}]. \tag{42}$$

Obviously $\det(\boldsymbol{J})$ is maximized if $\cos\theta_{12} = 0$, when the two UAVs measure the range and angle of the target in three-dimensional space, two UAVs should be as close to the target as possible and keep the line of sight angle $\theta_{12} = \pi/2$, so that the determinant of FIM gets the maximum and the target tracking error is the smallest. Fig. 2 shows the optimal observation geometry configuration of two UAVs.

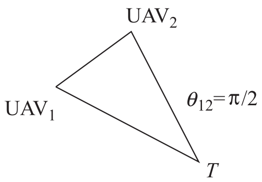

Fig. 2 Optimal observation geometry configuration of two UAVs

Equation (41) is proved as follows.

Proof According to the analysis of Section 2.2, let $N = 2$, the total determinant of FIM is computed as follows:

$$\det(\boldsymbol{J}_2) =$$
$$\frac{1+[\cos\varphi_1\cos\varphi_2\cos(\beta_1-\beta_2)+\sin\varphi_1\sin\varphi_2]^2}{\sigma_r^2\sigma^4R_1^4}+$$
$$\frac{1+[\cos\varphi_1\cos\varphi_2\cos(\beta_1-\beta_2)+\sin\varphi_1\sin\varphi_2]^2}{\sigma_r^2\sigma^4R_2^4}+$$
$$\frac{[\sin\varphi_1\cos\varphi_2\cos(\beta_1-\beta_2)-\cos\varphi_1\sin\varphi_2]^2}{\sigma_r^4\sigma^2R_1^2}+$$
$$\frac{\cos^2\varphi_2\sin^2(\beta_2-\beta_1)}{\sigma_r^4\sigma^2R_1^2}+$$
$$\frac{[\sin\varphi_2\cos\varphi_1\cos(\beta_1-\beta_2)-\cos\varphi_2\sin\varphi_1]^2}{\sigma_r^4\sigma^2R_2^2}+$$
$$\frac{\cos^2\varphi_1\sin^2(\beta_2-\beta_1)}{\sigma_r^4\sigma^2R_2^2}+$$
$$\frac{[\sin\varphi_1\cos\varphi_2-\cos\varphi_1\sin\varphi_2\cos(\beta_1-\beta_2)]^2}{\sigma^6R_1^4R_2^2}+$$
$$\frac{\cos^2\varphi_1\sin^2(\beta_2-\beta_1)}{\sigma^6R_1^4R_2^2}+$$
$$\frac{[\sin\varphi_2\cos\varphi_1-\cos\varphi_2\sin\varphi_1\cos(\beta_1-\beta_2)]^2}{\sigma^6R_1^2R_2^4}+$$
$$\frac{\cos^2\varphi_2\sin^2(\beta_2-\beta_1)}{\sigma^6R_1^2R_2^4}+$$
$$\frac{2\sin^2\varphi_1\sin^2(\beta_1-\beta_2)}{\sigma_r^2\sigma^4R_1^2R_2^2}+\frac{2\sin^2\varphi_2\sin^2(\beta_1-\beta_2)}{\sigma_r^2\sigma^4R_1^2R_2^2}+$$
$$\frac{2\cos^2(\beta_1-\beta_2)}{\sigma_r^2\sigma^4R_1^2R_2^2}+$$
$$\frac{2[\sin\varphi_1\sin\varphi_2\cos(\beta_1-\beta_2)+\cos\varphi_1\cos\varphi_2]^2}{\sigma_r^2\sigma^4R_1^2R_2^2}. \tag{43}$$

Let $\boldsymbol{r}(\varphi_i,\beta_i) = (\cos\varphi_i\sin\beta_i, \cos\varphi_i\cos\beta_i, \sin\varphi_i)$, we can get

$$\cos\theta_{12} = \boldsymbol{r}(\varphi_1,\beta_1)\boldsymbol{r}(\varphi_2,\beta_2) =$$
$$\cos\varphi_1\cos\varphi_2\cos(\beta_2-\beta_1)+\sin\varphi_1\sin\varphi_2, \tag{44}$$

$$[\cos\varphi_2\sin\varphi_1-\sin\varphi_2\cos\varphi_1\cos(\beta_2-\beta_1)]^2+$$
$$\cos^2\varphi_1\sin^2(\beta_2-\beta_1) =$$
$$1-[\boldsymbol{r}(\varphi_1,\beta_1)\boldsymbol{r}(\varphi_2,\beta_2)]^2 =$$
$$1-\cos^2\theta_{12}, \tag{45}$$

$$\sin^2\varphi_1\sin^2\varphi_2\cos^2(\beta_1-\beta_2) =$$
$$(1-\cos^2\varphi_1)(1-\cos^2\varphi_2)\cos^2(\beta_1-\beta_2) =$$
$$(\sin^2\varphi_1+\sin^2\varphi_2-1+\cos^2\varphi_1\cos^2\varphi_2)\cos^2(\beta_1-\beta_2) =$$
$$\sin^2\varphi_1[1-\sin^2(\beta_1-\beta_2)]+\sin^2\varphi_2[1-\sin^2(\beta_1-\beta_2)]-$$
$$\cos^2(\beta_1-\beta_2)+\cos^2\varphi_1\cos^2\varphi_2\cos^2(\beta_1-\beta_2). \tag{46}$$

From (46), we can get

$$\sin^2\varphi_1\sin^2\varphi_2\cos^2(\beta_1-\beta_2)+\sin^2\varphi_1\sin^2(\beta_1-\beta_2)+$$
$$\sin^2\varphi_2\sin^2(\beta_1-\beta_2)+\cos^2(\beta_1-\beta_2) =$$
$$\sin^2\varphi_1+\sin^2\varphi_2+\cos^2\varphi_1\cos^2\varphi_2\cos^2(\beta_1-\beta_2). \tag{47}$$

$$\cos^2\varphi_1\cos^2\varphi_2 =$$
$$(1-\sin^2\varphi_1)(1-\sin^2\varphi_2) =$$
$$1-\sin^2\varphi_1-\sin^2\varphi_2+\sin^2\varphi_1\sin^2\varphi. \tag{48}$$

From (48), we can get

$$\sin^2\varphi_1+\sin^2\varphi_2+\cos^2\varphi_1\cos^2\varphi_2=1+\sin^2\varphi_1\sin^2\varphi_2. \quad (49)$$

Substituting (44), (45), (47) and (49) into (43), we obtain (41) as follows:

$$\det(\boldsymbol{J}_2)=\det(\boldsymbol{F}_2)\det(\boldsymbol{F}_2^{\mathrm{T}})=\frac{(1+\cos^2\theta_{12})}{\sigma_r^2\sigma^4}\left(\frac{1}{R_1^4}+\frac{1}{R_2^4}\right)+\frac{(1-\cos^2\theta_{12})}{\sigma_r^4\sigma^2}\left(\frac{1}{R_1^2}+\frac{1}{R_2^2}\right)+\frac{(1-\cos^2\theta_{12})}{\sigma^6}\left(\frac{1}{R_1^2R_2^4}+\frac{1}{R_1^4R_2^2}\right)+\frac{2(1+\cos^2\theta_{12})}{\sigma_r^2\sigma^4R_1^2R_2^2}. \qquad \square$$

3.3 Analysis of optimal observation configuration for $N=3$

Let $F(i,j)$ be a function of (i,j) $(i,j\in\mathbf{N}^+)$ and

$$F(i,j)=\frac{(1+\cos^2\theta_{ij})}{\sigma_r^2\sigma^4}\left(\frac{1}{R_i^4}+\frac{1}{R_j^4}\right)+\frac{(1-\cos^2\theta_{ij})}{\sigma_r^4\sigma^2}\left(\frac{1}{R_i^2}+\frac{1}{R_j^2}\right)+\frac{(1-\cos^2\theta_{ij})}{\sigma^6}\left(\frac{1}{R_i^2R_j^4}+\frac{1}{R_i^4R_j^2}\right)+\frac{2(1+\cos^2\theta_{ij})}{\sigma_r^2\sigma^4R_i^2R_j^2}. \quad (50)$$

Let $E(i,j,k)$ be a function of (i,j,k) $(i,j,k\in\mathbf{N}^+)$ and

$$E(i,j,k)=\frac{2}{\sigma^6R_i^2R_j^2R_k^2}(1-\cos\theta_{ij}\cos\theta_{ik}\cos\theta_{jk})+\frac{1}{\sigma_r^4\sigma^2R_i^2}(\cos^2\theta_{ij}+\cos^2\theta_{ik}-2\cos\theta_{ij}\cos\theta_{ik}\cos\theta_{jk})+\frac{1}{\sigma_r^4\sigma^2R_j^2}(\cos^2\theta_{ij}+\cos^2\theta_{jk}-2\cos\theta_{ij}\cos\theta_{ik}\cos\theta_{jk})+\frac{1}{\sigma_r^4\sigma^2R_k^2}(\cos^2\theta_{ik}+\cos^2\theta_{jk}-2\cos\theta_{ij}\cos\theta_{ik}\cos\theta_{jk})+\frac{1}{\sigma_r^2\sigma^4R_i^2R_j^2}(1-\cos^2\theta_{ij}+2\cos\theta_{ij}\cos\theta_{ik}\cos\theta_{jk})+\frac{1}{\sigma_r^2\sigma^4R_i^2R_k^2}(1-\cos^2\theta_{ik}+2\cos\theta_{ij}\cos\theta_{ik}\cos\theta_{jk})+\frac{1}{\sigma_r^2\sigma^4R_j^2R_k^2}(1-\cos^2\theta_{jk}+2\cos\theta_{ij}\cos\theta_{ik}\cos\theta_{jk})+\frac{1}{\sigma_r^6}(1-\cos^2\theta_{ij}-\cos^2\theta_{ik}-\cos^2\theta_{jk}+2\cos\theta_{ij}\cos\theta_{ik}\cos\theta_{jk}). \quad (51)$$

When $N=3$, that is, three UAVs observe the target, the total determinant of FIM is

$$\det(\boldsymbol{J})=\det(\boldsymbol{J}_3)\det(\boldsymbol{J}_3^{\mathrm{T}})=\sum_{1\leqslant i<j\leqslant 3}F(i,j)+\sum_{1\leqslant i<j<k\leqslant 3}E(i,j,k). \quad (52)$$

The process of proof refers to $N=2$.

From (52), we can get when three UAVs observe, $R_i=r_{\min}$ $(i\in\{1,2,3\})$ is a necessary condition for the maximum determinant of FIM. When $R_1=R_2=R_3=r_{\min}$,

$$\det(\boldsymbol{J})=\frac{1}{\sigma_r^6\sigma^6r_{\min}^6}\{(\sigma^6r_{\min}^6+6\sigma_r^2\sigma^4r_{\min}^4+15\sigma_r^4\sigma^2r_{\min}^2+8\sigma_r^6)-(\sigma^2r_{\min}^6+5\sigma_r^4\sigma^2r_{\min}^2+2\sigma^6)(\cos^2\theta_{12}+\cos^2\theta_{13}+\cos^2\theta_{23})+[2(\sigma^4r_{\min}^4+3\sigma_r^4)(\sigma^2r_{\min}^2-3\sigma_r^2)+16\sigma_r^6]\cos\theta_{12}\cos\theta_{13}\cos\theta_{23}\}. \quad (53)$$

The problem is transformed into finding the extreme value of (53). It can be obtained that (53) achieves the maximum value when $\theta_{12}=\theta_{13}=\theta_{23}=\pi/2$, so when the three UAVs observe a single target, the optimal observation configuration between the three UAVs is $\theta_{12}=\theta_{13}=\theta_{23}=\pi/2$. Fig. 3 shows the optimal observation geometry configuration of three UAVs. When the distance between the UAV and the target is r, the distance between UAVs is $\sqrt{2}r$.

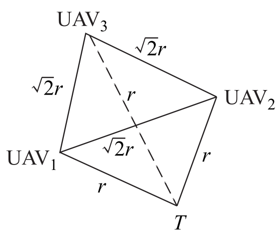

Fig. 3 Optimal observation geometry configuration of three UAVs

3.4 Analysis of optimal observation configuration for $N\geqslant 4$

The total determinant of FIM for $N\geqslant 4$ is

$$\det(\boldsymbol{J})=\det(\boldsymbol{J}_N)\det(\boldsymbol{J}_N^{\mathrm{T}})=\sum_{1\leqslant i<j\leqslant N}F(i,j)+\sum_{1\leqslant i<j<k\leqslant N}E(i,j,k). \quad (54)$$

When there is a minimum observation distance $R_i = r_{\min}$ $(i \in \{1, 2, \ldots, N\})$, maximizing (54) is equivalent to minimizing

$$\sum_{1\leqslant i<j\leqslant N} a\cos^2\theta_{ij} - \sum_{1\leqslant i<j<k\leqslant N} b\cos\theta_{ij}\cos\theta_{ik}\cos\theta_{jk} \tag{55}$$

where a and b are constants about $r_{\min}$, σ_r and σ [23].

When the sea surface target is measured by N UAVs, the problem becomes how to distribute N UAVs on the hemisphere with the target as the center to minimize (55). Some studies on the problem of optimally arranging points on a sphere that maximize or minimize some quantity are still unsolved [24], so it is a worldwide problem.

Through observation, we can see that (55) is an expression with strict symmetry, and it is conjectured that the geometric configuration maximizing (55) is also strictly symmetrical. One possible geometric configuration is that N UAVs are uniformly distributed on the hemispheric surface. Unfortunately, the strict mathematical proof cannot be given yet, which is the direction of future work.

4. Cooperative target tracking

The problem of two UAVs cooperating on target tracking is considered [25], and the UAV flies at the same altitude. According to the analysis of the optimal observation configuration of two UAVs, we can get from (42) that

$$[R_1, R_2, \theta_{12}] = \arg\max_{\substack{R_1,R_2\in[r_{\min},-\infty)\\ \theta_{12}\in[0,\pi]}} \det(\boldsymbol{J}_2) = [r_{\min}, r_{\min}, \pi/2]. \tag{56}$$

Equation (56) shows that when two UAVs are as close as possible to the safe observation distance and maintain a line of sight angle of $\pi/2$, the target tracking error is the smallest, and the target state estimation is more accurate.

4.1 Optimal observation control for cooperative target tracking

The optimal control method is designed to make the angle between UAVs and the target close to or maintain at 90° in three-dimensional space, so as to improve the accuracy and real-time performance of target tracking.

It is only necessary to design the control method in the approaching phase because the UAV is far away from the target and is close to the target motion for over-the-horizon target tracking. In order to reach the line of sight angle of 90°, the heading angle control of UAVs [26–28] is designed as follows:

$$\begin{cases} \alpha_1 = \beta_1 + k_1(\theta_{12})\sin(\theta_{12} - \pi/2) \\ \alpha_2 = \beta_2 - k_2(\theta_{12})\sin(\theta_{12} - \pi/2) \end{cases}. \tag{57}$$

According to (35)

$$\theta_{12} = \arccos(\cos\varphi_1\cos\varphi_2\cos(\beta_1 - \beta_2) + \sin\varphi_1\sin\varphi_2). \tag{58}$$

The β_1 and β_2 components guide the UAV to fly to the target and shorten the distance to the target, the $\sin(\theta_{12} - \pi/2)$ component makes the line-of-sight angle between the two UAVs and the target approach 90°. Adjust the degree of tending to 90° through proportional coefficients $k_1(\theta_{12})$ and $k_2(\theta_{12})$.

$$\begin{cases} k_1(\theta_{12}) = K_1 \cdot |\sin(\theta_{12} - \pi/2)| \\ k_2(\theta_{12}) = K_2 \cdot |\sin(\theta_{12} - \pi/2)| \end{cases} \tag{59}$$

where K_1 and K_2 are proportional coefficients.

$$K_1 = \begin{cases} \dfrac{D}{D_1 - r_{\min}}, & \dfrac{D}{D_1 - r_{\min}} < 1.21 \\ 1.21, & \text{otherwise} \end{cases},$$

$$K_2 = \begin{cases} \dfrac{D}{D_2 - r_{\min}}, & \dfrac{D}{D_2 - r_{\min}} < 1.21 \\ 1.21, & \text{otherwise} \end{cases},$$

where D is a distance factor; D_1 and D_2 are the distance from two UAVs to the target respectively; and $r_{\min}$ represents the minimum safe observation distance. When it is far from the target, increase the control amount of UAV in the direction of the target movement to approach the target. When it is close, increase the control amount of the angle between the UAV and the target line of sight to achieve the optimal observation angle.

4.2 Fusion filtering algorithm

In order to make effective use of observation information and reduce the impact of observation errors on positioning accuracy, a certain filtering algorithm is needed. In this paper, the classical extended Kalman filter (EKF) algorithm is used to filter the observation data of UAV.

Assume that two UAVs get two trajectories i and j after EKF with state estimates $\widehat{\boldsymbol{x}}_i$ and $\widehat{\boldsymbol{x}}_j$, error covariances $\boldsymbol{P}_i$ and $\boldsymbol{P}_j$. The purpose of estimation fusion is to find the best estimate $\widehat{\boldsymbol{x}}$ and error covariance matrix $\boldsymbol{P}$.

$$\widehat{\boldsymbol{x}} = \boldsymbol{P}_j(\boldsymbol{P}_i + \boldsymbol{P}_j)^{-1}\widehat{\boldsymbol{x}}_i + \boldsymbol{P}_i(\boldsymbol{P}_i + \boldsymbol{P}_j)^{-1}\widehat{\boldsymbol{x}}_j = \boldsymbol{P}(\boldsymbol{P}_i^{-1}\widehat{\boldsymbol{x}}_i + \boldsymbol{P}_j^{-1}\widehat{\boldsymbol{x}}_j) \tag{60}$$

$$\boldsymbol{P} = \boldsymbol{P}_i(\boldsymbol{P}_i + \boldsymbol{P}_j)^{-1}\boldsymbol{P}_j = (\boldsymbol{P}_i^{-1} + \boldsymbol{P}_j^{-1})^{-1} \tag{61}$$

5. Numerical simulation and analysis

It is assumed that the target is moving with a constant speed at 8 m/s and direction at $\pi/4$, the initial position of the target is at (0 m, 200 000 m, 0 m). The speeds of UAVs are 100 m/s with the fly attitude at 2 500 m. The initial positions of UAV_1 and UAV_2 are (12 500 m, 48 412 m, 2 500 m) and (−12 500 m, 48 412 m, 2 500 m) respectively. The random and system errors of sensors are (1 m, 0.05°, 0.05°) and (3 m, 0.1°, 0.1°) with random error obeying Gauss distribution. The minimum safe distance is $r_{\min} = 50$ km and the entire simulation lasts 1 250 s. The simulation results are shown in Figs. 4–7. In Fig. 4, $*$ and Δ represent the initial position of the UAV and the target, respectively.

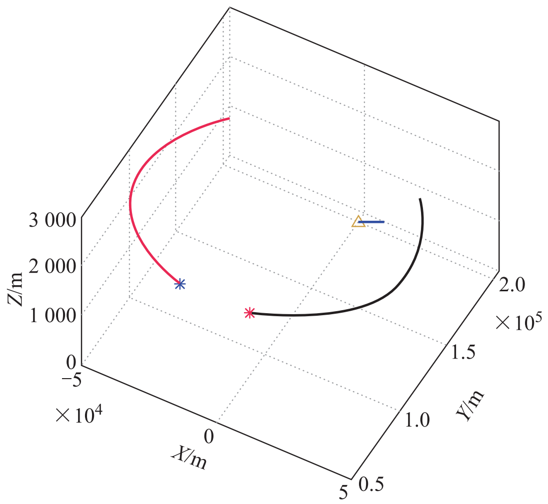

(a) Trajectory of UAVs and target in three-dimensional space

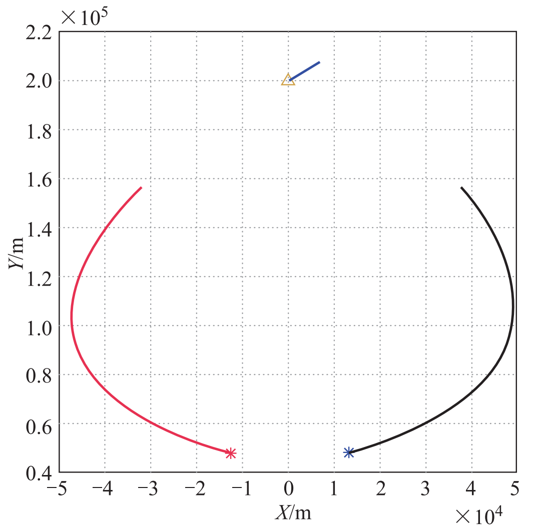

(b) Trajectory of UAVs and target in two-dimensional space

: UAV_1 trajectory; : UAV_2 trajectory;
: Target trajectory.

Fig. 4 Trajectory of UAVs and target

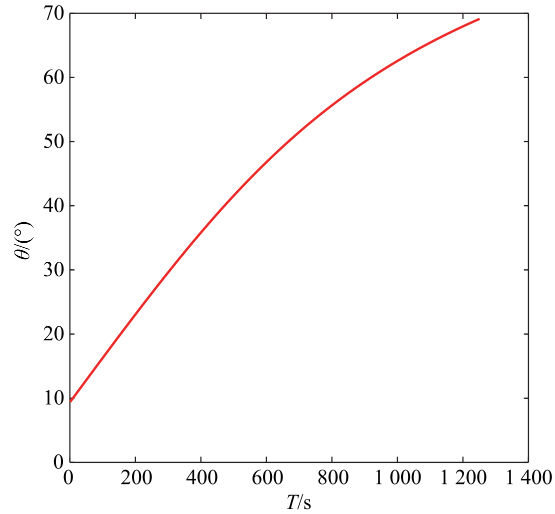

Fig. 5 Angle of sight between UAVs and target

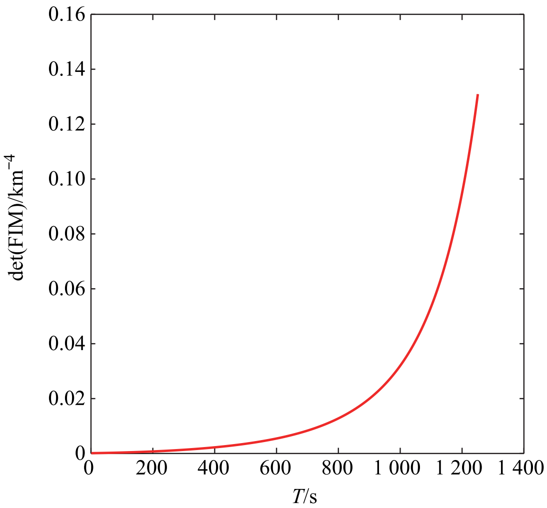

Fig. 6 Determinant of FIM

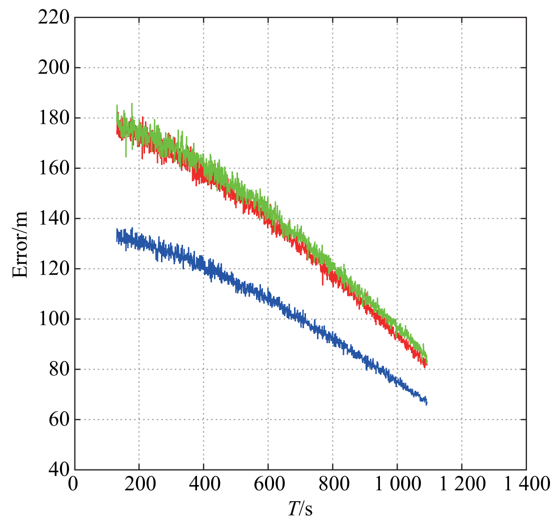

: Tracking error of UAV_1; : Tracking error of UAV_2;
: Cooperative tracking error.

Fig. 7 Tracking error of the target

From the simulation results, it can be seen that the two UAVs separate a certain angle when tracking as shown in Fig. 4, and the line-of-sight angle between the UAVs and the target increases as shown in Fig. 5. As the UAVs approach the target and the line-of-sight angle increases, the determinant of the system FIM becomes larger as shown in Fig. 6, the error of the target state which the UAV estimates is smaller as shown in Fig. 7, and the target positioning is more accurate.

Through the analysis of Fig. 6, the change rate of the determinant of FIM is getting larger as a result of the UAV is getting closer to the target, and it can be derived from (41). Combined with Fig. 5, although the line-of-sight angle between the UAVs and the target increases slowly with time, it has little effect on the growth rate of the determinant of FIM. Therefore, it is necessary to make the UAV close to the target as soon as possible under the condition that the line-of-sight angle approaches 90°.

As seen from Fig. 7, the target error observed by UAV_1 is 196.2 m at the initial time, and the target error of cooperative tracking observation by two UAVs is 133.4 m, which improves the error accuracy by 32%. Therefore, compared with the single UAV, it can effectively improve the positioning accuracy of the target by two UAVs' observations. Moreover, the cooperative tracking error of the target is 133.4 m at the initial time in Fig. 7, and the cooperative tracking error is 56.2 m at 1 250 s, which improves the tracking error accuracy by 58%. It can be concluded that the theory analyzed in this paper and the proposed control algorithm can effectively improve the positioning accuracy of the over-the-horizon target.

6. Conclusions and future work

In this paper, the problem of optimal configuration based on range and angle measurements is extended from two-dimensional space to three-dimensional space, which can be widely used in military and engineering fields. This paper focuses on the observation model of sensors based on range and angle measurements and takes the FIM determinant of UAV observation in three-dimensional space as the cost function. The expression of optimal observation geometry and the conditions of optimal configuration solution of UAVs observation are given. It is pointed out that the optimal observation configuration is usually not unique. The optimal control method of cooperative target tracking by two UAVs is proposed based on the analysis of optimal observation configuration of the two UAVs. The simulation results show that the theoretical analysis and the control algorithm in this paper can effectively improve the positioning accuracy of the over-the-horizon target.

However, only an optimal control method for cooperative tracking of two UAVs is proposed, how to realize the optimal observation control of three or more UAVs is the focus of the next research. Moreover, when using UAVs as the observation platform to estimate the target state, we should also consider the influence of the UAV attitude angle accuracy on the tracking error. How to improve the accuracy of the UAV attitude angle is also the next research direction.

References

[1] BAI T, WANG D. Cooperative trajectory optimization for unmanned aerial vehicles in a combat environment. Science China: Information Sciences, 2019, 62(1): 52 – 54.
[2] KOYUNCU E, SHABANIGHAZIKELAYEH M, SEFEROGLU H. Deployment and trajectory optimization of UAVs: a quantization theory approach. Proc. of the IEEE Wireless Communications and Networking Conference, 2018: 1 – 6.
[3] XU C, HUANG D Q. Error analysis for target localization with unmanned aerial vehicle electro-optical detection platform. Chinese Journal of Scientific Instrument, 2013, 34(10): 2265 – 2270. (in Chinese)
[4] SHAO H. Research on high precision target localization technology in UAV. Nanjing, China: Nanjing University of Aeronautics and Astronautics, 2014. (in Chinese)
[5] PACK D, YORK G, FIERRO R. Information-based cooperative control for multiple unmanned aerial vehicles. Proc. of the IEEE International Conference, 2006. DOI: 10.1109/ICNSC.2006.1673187.
[6] CAMPBELL M E, WHITACRE W W. Cooperative tracking using vision measurements on seascan UAVs. IEEE Trans. on Control Systems Technology, 2007, 15(4): 613 – 627.
[7] WANG L, PENG H, ZHU H Y, et al. Cooperative tracking of ground moving target using unmanned aerial vehicles in cluttered environment. Control Theory & Applications, 2011, 28(3): 300 – 308. (in Chinese)
[8] YU Z J, SUN Y R, ZHU Y F, et al. High precision algorithm of dual-aircraft cooperative locating with angle and distance Information. Ordnance Industry Automation, 2019, 38(2): 1 – 5. (in Chinese)
[9] ZHAO S, CHEN B M, LEE T H. Optimal sensor placement for target localization and tracking in 2D and 3D. International Journal of Control, 2013, 86(10): 1687 – 1704.
[10] LEE W, BANG H, LEEGHIM H. Cooperative localization between small UAVs using a combination of heterogeneous sensors. Aerospace Science and Technology, 2013, 27(1): 105 – 111.
[11] MORENO S, ALIMS D, PASCOAL A M, et al. Optimal sensor placement for multiple target positioning with range-only measurements in two-dimensional scenarios. Sensors, 2013, 13(8): 10674 – 10710.
[12] TICHAVSKY P, MURAVCHIK C H. Posterior Cramer-Rao bounds for discrete-time nonlinear filtering. IEEE Trans. on Signal Processing, 1998, 46(5): 1386 – 1395.
[13] ADRIAN N B, BARIS F, BRIAN D O A, et al. Optimality analysis of sensor-target localization geometries. Automatica, 2010, 46(3): 479 – 492.
[14] SAMEERA S P. Trajectory optimization for target localization using small unmanned aerial vehicles. Proc. of the AIAA Guidance, Navigation, and Control Conference, 2009: 1 – 25.
[15] SONIA M, FRANCESCO B. Optimal sensor placement and motion coordination for target tracking. Automatica, 2006, 42(4): 661 – 668.

[16] ERIC W F. Sensitivity of cooperative target geolocalization to orbit coordination. Journal of Guidance, Control, and Dynamics, 2008, 31(4): 1028 – 1040.
[17] WANG L. Modeling and optimization for multi-UAVs cooperative target tracking. Changsha, China: National University of Defense Technology, 2011. (in Chinese)
[18] ZHONG Y, WU X Y, HUANG S C, et al. Optimality analysis of sensor-target geometries for bearing-only passive localization in three-dimensional space. Chinese Journal of Electronics, 2016, 25(2): 391 – 396.
[19] LOGOTHETIS A, ISAKSSON A, EVANS R J. An information theoretic approach to observer path design for bearings-only tracking. Proc. of the 36th IEEE Conference on Decision and Control, 1997: 3132 – 3137.
[20] FREW E W. Observer trajectory generation for target-motion estimation using monocular vision. California, America: Stanford University, 2003.
[21] ZHOU K, ROUMELIOTIS S I. Optimal motion strategies for range-only constrained multi-sensor target tracking. IEEE Trans. on Robotics, 2008, 24(5): 1168 – 1185.
[22] YAO M S. Higher algebra. Shanghai: Fudan University Press, 2003. (in Chinese)
[23] JORGE N, STEPHEN J W. Numerical optimization. 2nd ed. New York: Springer Science Business Media, 2006.
[24] HOU X R, SHAO J W. Spherical distribution of 5 points with maximal distance sum. Discrete and Computational Geometry, 2011, 46(1): 156 – 174.
[25] ZHANG S H, YANG J D, ZHANG H L, et al. Dual trajectory optimization for a cooperative internet of UAVs. IEEE Communications Letters, 2019, 23(6): 1093 – 1096.
[26] ZHONG C M, ZHAO Z Y, SUN H B, et al. A closed-loop optimal control for multiple unmanned aerial vehicles cooperative target tracking. Journal of Detection & Control, 2012, 34(3): 13 – 18. (in Chinese)
[27] DI B. Key issues in reconnaissance-oriented cooperative control of multiple unmanned aerial vehicles. Beijing, China: Beijing University of Aeronautics and Astronautics, 2015. (in Chinese)
[28] LIU Z, GAO X G, FU X W. Co-optimization of communication and observation for multiple UAVs in cooperative target tracking. Control and Decision, 2018, 33(10): 1747 – 1756. (in Chinese)

Biographies

SHI Haoran was born in 1992. He received his M.E. degree from Naval Aeronautical and Astronautical University. Now he is a Ph.D. candidate of the College of Weaponry Engineering, Naval University of Engineering. His research interests include systems and control, optimization theory and target localization and tracking by UAVs.
E-mail: Shihaoran_1992@163.com

LU Faxing was born in 1974. He received his M.E. degree from Naval University of Engineering in 2000 and Ph.D. degree from Naval Academy of Kuznetsov in 2008. Now he is an associate professor at Naval University of Engineering. His research interests include command and control.
E-mail: lfx1974@163.com

WANG Hangyu was born in 1965. He received his M.E. and Ph.D. degrees from Naval University of Engineering in 1994 and 2004, respectively. Now he is a professor at Naval University of Engineering. His research interests include fields of command and control.
E-mail: wanghangyu@sina.com

XU Junfei was born in 1990. He received his M.E. and Ph.D. degrees from Naval University of Engineering in 2015 and 2019, respectively. Now he is a lecturer at Naval University of Engineering. His research interests include optimization theory and application.
E-mail: xjf09531@sina.com